Design and testing of planting unit for rice dry-direct-seeding planter in cold region

Jiale Zhao[1], Chengliang Zhang[1,2*], Yanpeng Wei[1], Mingzhuo Guo[3*], Chao Chen[4], Chongqin Zhang[4], Yungan Zhang[5]

(1. *Key Laboratory of Bionics Engineering, Ministry of Education, Jilin University, Changchun 130025, China*;
2. *Harbin Academy of Agricultural Sciences, Harbin 150029, China*;
3. *College of Biological and Agricultural Engineering, Jilin University, Changchun 130025, China*;
4. *Weichai Lovol Intelligent Agricultural Technology Co., Ltd., Weifang 261200, China*;
5. *School of Mechanical Engineering, University of Jinan, Jinan 250022, China*)

Abstract: Rice dry-direct-seeding technology is a time-saving, cost-saving and efficient rice cultivation technique that increases the efficiency of seeding. In order to implement the specialization, light simplicity and scale of rice production, improve the level of mechanization of the whole rice production process, and solve the problems of uneven seed furrows, uneven number of seeds sown, shallow mulching and uncompact repression that occur during the promotion and application of dry-direct-seeding for rice in the cold region of northeast China. In this paper, a planting unit for rice dry-direct-seeding planter is designed. The working principles and structural parameters of the furrow opening components, the seeding apparatus and the soil covering-pressing device are described. The mechanical model of the key components of the seeding unit was established, and the forward speed, roller diameter and compacting strength were selected as the test factors. A three-factor, five-level quadratic rotation orthogonal combination test was conducted with the seed breakage rate, seeding depth qualification rate, seeding uniformity coefficient of variation and hole grain count qualification rate as the evaluation indexes. Field performance test and test results show that: at a forward speed of 4 km/h, a roller diameter of 427 mm and a compacting strength of 48.45 kPa, the seed breakage rate was 1.31%, the sowing depth qualification rate was 9.95%, the coefficient of variation of sowing uniformity was 3.75% and the number of holes was 86.75%. This accords with the agronomic requirements of dry-direct-seeding for rice and implements a combination of superior agronomy and modern farm machinery.

Keywords: rice, dry-direct-seeding, planting unit, structural design, testing research
DOI: 10.25165/j.ijabe.20231604.7843

Citation: Zhao J L, Zhang C L, Wei Y P, Guo M Z, Chen C, Zhang C Q, et al. Design and testing of planting unit for rice dry-direct-seeding planter in cold region. Int J Agric & Biol Eng, 2023; 16(4): 76–84.

1 Introduction

As one of the world's most important food crops, rice is grown in the monsoon and tropical rainforest regions of East, Southeast and South Asia[1,2]. China is the largest rice producer in the world. In 2019, the planting area is 30.76 thousand hm^2, and the rice yield is 21.86 million t, accounting for about 32% of the world's total rice production[3,4].

At present, rice cultivation in China is still dominated by seedling cultivation, transplanting and irrigation, with low levels of cultivation mechanisation, low operational efficiency and serious wastage of water resources[5-7]. Dry-direct seeding for rice is a water-saving cultivation technique in which the land is prepared in a dry field state, the treated rice seeds are sown directly into the rice field, and the field is wetted by drip irrigation after sowing, with no or little irrigation in the early stage and scientific and reasonable irrigation in the later stage according to the law of rice physiological water demand[8-11].

The rice growing area in the cold north-eastern region of China is flat and vast and suitable for large scale mechanized operations. However, due to the constraints of lower temperatures, shorter light hours, lack of water resources and backward supporting farm machinery and agronomic techniques, dry-direct-seeding technology for rice has not been applied in a large scale[12-14].

To address the problems of poor stability of the depth and width of the seed furrow, poor uniformity and high volatility of seed discharge, low performance of mulching, soil breaking and suppression in the application of dry-direct-seeding machines for rice in cold regions[15-18]. In this paper, a planting unit suitable for dry-direct-seeding of rice in cold regions of northeast China is developed with reference to the actual agricultural conditions of rice cultivation and the agronomic requirements of dry-direct-seeding technology for rice. This planting unit can complete the entire planting process of trenching, seeding and mulching in one operation.

Received date: 2022-08-05 **Accepted date:** 2023-03-18
Biographies: Jiale Zhao, PhD, Professor, research interest: bionic intelligent agricultural machinery and conservation tillage, Email: zhaojiale0313@163.com; **Yanpeng Wei**, PhD, research interest: agricultural machinery and conservation tillage technology, Email: china_dp@163.com; **Chao Chen**, PhD, research interest: agricultural machinery and conservation tillage, Email: chenchao-l@lovol.com; **Chongqin Zhang**, PhD, research interest: agricultural machinery and conservation tillage technology, Email: zhangchongqin@lovol.com; **Yungan Zhang**, PhD, research interest: agricultural machinery and conservation tillage, Email: zhangyungan2023@163.com.
***Corresponding author: Chengliang Zhang**, PhD, research interest: intelligent ploughing machinery and equipment design. Harbin Academy of Agricultural Sciences, Harbin 150029, China. Tel: +86-15244621535, Email: obama1@163.com; **Mingzhuo Guo**, PhD, research interest: bionic intelligent agricultural machinery. School of Biological and Agricultural Engineering, Jilin University, Changchun 130022, China. Tel: +86-18504311293, Email: guomingzhuo@outlook.com.

This paper focuses on the structural principle and mechanical characteristics of dry-direct-seeding units for rice in cold regions, and investigates the stresses, movement laws and operational effects of seeding units through a combination of theoretical numerical analysis and field tests. This paper provides theoretical references for the optimal design of rice dry seeding machines in cold regions.

2 Structure and working principle of planting unit

The dry-direct-seeding unit for rice in cold regions mainly consists of imitation institutions, ditchers, seed meters, hillers and pressing rollers. The overall structure is shown in Figure 1.

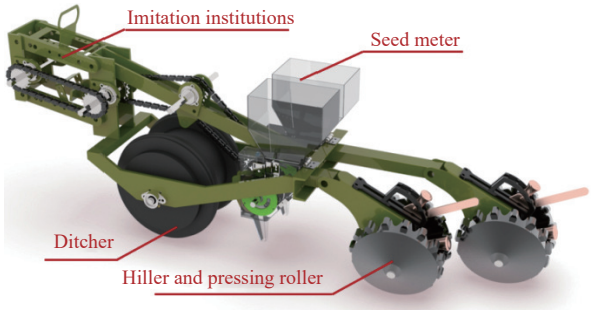

Figure 1 General structure of the planting unit

The planting unit is attached to the crossbeam of the dry-direct-seeding machine for rice by means of the fixing seat of the imitation institutions. The dry-direct-seeding machinery for rice is connected to the tractor by means of a standard three-point suspension. When working, the tractor pulls the dry-direct-seeding machinery for rice forward, the parallel four-bar imitation institutions control the depth of furrow opening and seeding depth, the ditcher presses out the seed furrow through the rotating pressure roller, the ground wheel drives the seed rower through the chain drive to sow the rice seeds into the seed furrow at low speed, the soil covering-pressing device completes the suppressing and backfilling of the soil on the surface of the seeds in the seed furrow.

3 Design of key components

3.1 Design of the ditcher

3.1.1 Structural design of the ditcher

The ditcher is the working part of the planting unit to construct the seed furrow. A superior quality seed trench should compact the subsoil for water and moisture storage. The structure of the ditcher directly affects the quality of the seeding operation[19,20]. The dither consisting of frame and pressing roller s.

3.1.2 Mechanical model of the pressing roller s

When the pressing roller is in operation, the raised outer edge of the wheel touches the soil first, compacting the subsoil and pressing out the seed furrow. The different curvature of the wheel edge has a soil breaking and drag reducing effect. When the outer wheel edge is completely sunk into the soil, the inner roller comes into contact with the soil and suppresses the soil on both sides of the seedling belt. The radius of curvature of the outer wheel edge is small in relation to the diameter of the roller and is negligible for force analysis. At the same time, neglecting the relative sliding of the pressure roller in the soil and treating it as a rigid roller body that only performs pure rolling, the simplified force on the pressure roller is shown in Figure 2c.

As shown in Figure 2, z_0 is the maximum depth of penetration of the pressure roller into the soil; z is the depth of entry corresponding to any point B on the edge of the pressure roller; θ_0 is the angle of the center of the circle corresponding to the maximum depth of soil entry z_0; R is the radius of the pressure roller; P is the traction force on the pressure roller; W is the pressure generated by the pressure roller in the vertical direction; x is the horizontal coordinate corresponding to point B; dQ is the compressive reaction force of the soil acting in a tiny section dl on the wheel edge.

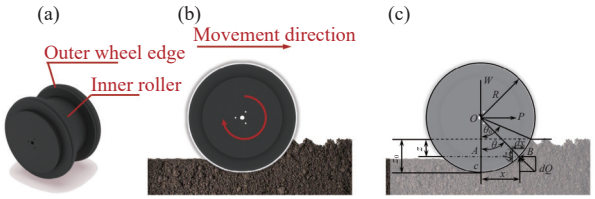

Figure 2 Structure of the pressure roller and the forces applied

During operation, the equilibrium equation of the pressure roller in the xoz plane is

$$\sum F_x = P - \int_0^{\theta_0} dQ \sin\theta = 0 \tag{1}$$

$$\sum F_z = W - \int_0^{\theta_0} dQ \cos\theta = 0 \tag{2}$$

Also because,

$$dQ = pbdl \tag{3}$$

where, p is the compacting strength of the soil; b is the width of the roller; dl is the arc length of a tiny section on the wheel edge.

Therefore,

$$P = \int_0^{\theta_0} pbdl\sin\theta = \int_0^{z_0} pbdz \tag{4}$$

$$W = \int_0^{\theta_0} pbdl\cos\theta = \int_0^{x} pbdx \tag{5}$$

where, $p = (\frac{k_c}{b} + k_\varphi)\cdot z^n$, k_c is a coefficient to be determined in relation to soil cohesion; k_φ is a coefficient to be determined in relation to soil friction; z is the depth of entry and n is the soil elastoplasticity index.

Then,

$$P = \int_0^{z_0} \left(\frac{k_c}{b} + k_\varphi\right)\cdot z^n bdz = (k_c + bk_\varphi)\cdot \frac{z_0^{n+1}}{n+1} \Rightarrow z_0 = \left[\frac{P(n+1)}{k_c + bk_\varphi}\right]^{\frac{1}{n+1}} \tag{6}$$

$$W = \int_0^{x} \left(\frac{k_c}{b} + k_\varphi\right)\cdot z^n bdx = (k_c + bk_\varphi)\int_0^{x} z^n dx \tag{7}$$

In ΔOAB, $AB^2 = OB^2 - OA^2$, namely $x^2 = R^2 - [R - (z_0 - z)]^2 \approx 2R(z_0 - z)$.

After differential, $dx = -\frac{rdz}{x} = -\frac{\sqrt{R}dz}{\sqrt{2(z_0 - z)}}$, therefore,

$$W = -\sqrt{\frac{R}{2}}\cdot\left(\frac{k_c}{b} + k_\varphi\right)\cdot b\int_{z_0}^{0}\frac{z^n}{z_0 - z}dz \approx \sqrt{2R}\cdot\left(\frac{k_c}{b} + k_\varphi\right)\cdot b\cdot\left[\frac{3-n}{3}(z_0)^{n+\frac{1}{2}}\right] \tag{8}$$

$$z_0 = \left[\frac{3W}{\sqrt{2R}\cdot(3-n)\cdot(k_c/b + k_\varphi)\cdot b}\right]^{\frac{2}{2n+1}} \tag{9}$$

The equation shows that the lower limit of the press roll is related to the load applied, the radius, the width and the soil characteristic coefficient. Therefore, the desired soil compactness of the seed substrate can be obtained by varying the construction size and weight of the pressing roller .

3.2 Design of the seeding apparatus

3.2.1 Structural design of the seeding apparatus

The seeding apparatus is the core working part of the dry-direct-seeding unit for rice. A well-structured seed planter is capable of steadily, accurately and evenly discharging rice seed into the seed furrow[21,22]. There are two forms of dry-direct-seeding for rice: strip sowing and hole sowing. In this paper, a combination of a spiral external grooved wheel seeding apparatus and a type-hole wheel seeding apparatus is used. This meets the sowing requirements for both strip and hole sowing and facilitates comparative trials[23,24]. The combined seeding apparatus consists of a seed box, shell, seed cleaning brush, tranmission shaft, seed release plate, seed rowing tube, combined seed rowing wheel, seed protection belt, seed limiting plate and seed adjusting plate. The structure of the seeding apparatus is shown in Figure 3.

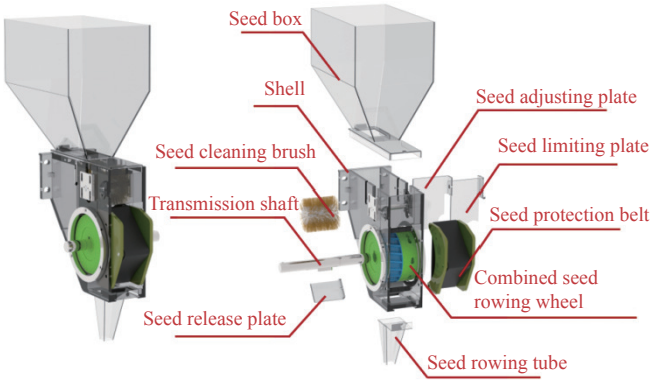

Figure 3 Structure of the seeding apparatus

3.2.2 Structural design of the combined seeding wheel

The combined seeding wheel consists of a spiral groove wheel and a type-hole wheel. When the key of the seed row shaft is connected to the spiral groove wheel, the groove wheel rotates to complete the strip sowing; when the key of the seed row shaft is connected to the type-hole wheel, the type hole wheel rotates to complete the hole sowing.

(1) The seeding quantity of the spiral grooved wheel is given by Equation (10)

$$q = \pi DL\gamma\left(\frac{kf}{t}+\lambda\right) \tag{10}$$

where, $t=\dfrac{\pi D}{z}$, q is the amount of fertilizer applied per revolution of the spiral groove wheel, g; D is the diameter of the spiral grooved wheel, cm; L is the effective working length of the spiral groove wheel, cm; γ is the seed density, g/cm^3; k is the seed filling factor; f is the cross-sectional area of the individual spiral grooves, cm^2; t is the spiral groove pitch, cm; z is the number of grooves; λ is the driving layer characteristic coefficient of seeds.

Due to the action of the seed discharge brush and seed guard belt, the slotted wheel drives a negligible amount of seed discharge, namely $\lambda = 0$.

Therefore,

$$q = L\gamma kfz \tag{11}$$

From Figure 4, the cross-sectional area of a single spiral groove can be derived from the following equation.

$$f = \left(S_{\text{Sector}O_1AB} - S_{\Delta O_1AB}\right) + \left(S_{\text{Sector}O_2AB} - S_{\Delta O_2AB}\right) = S_{\text{Sector}O_1AB} + S_{\text{Sector}O_2AB} - 2S_{\Delta O_1O_2B} \tag{12}$$

where, O_1O_2=O_2B=R (Groove wheel radius), O_1B=r (Spiral groove radius).

Therefore,

$$f = r^2\arccos\frac{r}{2R} + 2R^2\arcsin\frac{r}{2R} - r\sqrt{R^2-\frac{1}{4}r^2} \tag{13}$$

When $R \gg r$, $f \approx r^2\arccos\dfrac{r}{2R}$.

Substituting the corresponding coefficients and grooved roller dimensions into the above equation gives the following values: q_1=6.72 g (L=1 cm), q_2=13.44 g (L=2 cm), q_{max}=20.16 g (L_{max}= 3 cm).

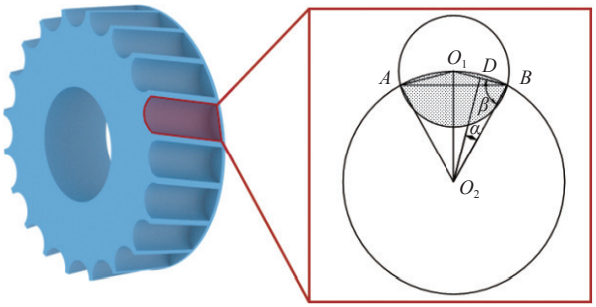

Figure 4 Schematic diagram of the cross-section of the spiral groove

(2) The structural parameters of the type hole are important to ensure the accuracy of the hole sowing. Rice seeds are shaped like ellipsoidal spheres and fill the type hole in three forms: flat, lateral and vertical[25,26], as shown in Figure 5.

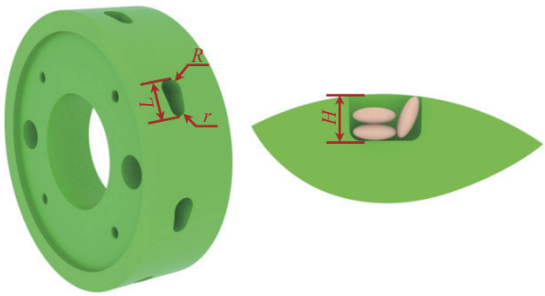

Figure 5 Structure of the type hole

The type hole consists of two circular arcs of radius R and r. To facilitate seed filling and sowing, the following equation should be satisfied.

$$\begin{cases} 2r \geq l_{max} \\ 2R \geq 1.1l_{max} \\ L \geq l_{max} + w_{max} \end{cases} \tag{14}$$

where, r is the small arc radius, mm; R is the large arc radius, mm; L is the total length of the type hole, mm; l_{max} is the maximum length of the rice seed, mm; w_{max} is the maximum width of the rice seed, mm; t_{max} is the maximum thickness of the rice seed, mm.

The depth of the type hole and the number of seed-filled grains per layer can be expressed by the following equation.

$$H = \frac{N}{n}\cdot t_{max} \tag{15}$$

$$n = \frac{R+r}{w_{max}} \tag{16}$$

where, H is the depth of the hole, mm; N is the number of seeds in the hole; n is the number of filled seeds per layer.

According to the agronomic requirements of dry-direct-seeding for rice in the cold regions of Northeast China, it is best to sow 5 to 7 seeds per hole. The dimensions of the rice seeds are as follows: lengths are mainly distributed between 6.1 and 9.1 mm, widths

between 2.6 and 3.5 mm and thicknesses between 2.0 and 2.6 mm[27-29]. By substituting the statistical values into the corresponding equations and after smoothing, the following type hole dimensions are obtained: the small arc radius is 4.5 mm, the large arc radius is 5 mm, the total length of the type hole is 13 mm and the depth of the type hole is 7 mm.

3.3 Design of the soil covering-pressing device

3.3.1 Structural design of the soil covering-pressing device

The soil covering-pressing device is a key component in the construction of the seed bed by the seeding unit. A high quality seed bed has a reasonable soil structure, with an even mulch and firm soil, which facilitates the growth and germination of the rice seed. In this paper, a self-rotating extruding soil covering-pressing device with soil breaking function is designed. The edge of the suppression roller engages at the bottom of the trench, the position and angle of engagement is adjustable and the protruding structure on the outside of the edge has both suppression and soil breaking functions. The soil covering-pressing device consists of a connecting frame, a soil covering-pressing wheel, an angle adjustment mechanism and a pressure adjustment mechanism. The structure of the the soil covering-pressing device is shown in Figure 6a.

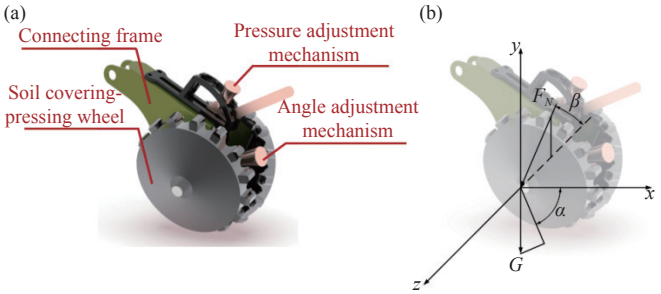

Figure 6 Force analysis of soil subjected to suppression

3.3.2 Modeling of the soil covering-pressing wheel

(1) Parameters of the soil covering-pressing wheel

The parameters of the soil covering-pressing device directly influence the suppression effect and slip rate. The smaller the diameter of the soil covering-pressing wheel, the greater the slip rate during operation, while soil dragging and soil congestion can occur. The conditions for proper operation and non-slip of the soil covering-pressing wheel are shown in the following equations.

$$R = \frac{h}{1-\cos\theta} \tag{17}$$

$$R \geq \frac{M_r}{Qf} \tag{18}$$

where, R is the radius of the overburden ballast wheel, mm; M_r is the frictional moment in the sleeve, N-m; Q is the total load on the overburden ballast wheel, N; f is the coefficient of friction between the soil and the overburden ballast wheel; h is the lower limit of the soil, mm; θ is the angle of the circle corresponding to the depth of entry h, (°).

In this paper, the structure of the outer edge of the soil covering-pressing wheel is effective in reducing the slip rate. The ditcher is capable of compacting the bottom of the trench during the construction of the seed trench. Therefore, the lower limit of the radius of the soil covering-pressing wheel, namely R = 128 mm, is desirable to meet normal operating conditions.

(2) Force analysis of the soil covering-pressing wheel

When the soil covering-pressing wheel is in operation, it can be considered a rigid body. The contact area between the soil covering-pressing wheel and the soil can be expressed as the product of the width of the rigid wheel and the radial contact arc length. The pressure exerted on the soil by the soil covering-pressing wheel can be expressed by the following equation.

$$p = \frac{F}{S} \tag{19}$$

where, $S = BR\arccos\frac{R-h}{R}$, p is the pressure exerted on the soil by the soil covering-pressing wheel during operation, kPa; F is the ballast pressure exerted on the soil by the soil covering-pressing wheel, N; S is the contact area between the soil covering-pressing wheel and the soil, mm^2.

As shown in Figure 6b, the ballast pressure generated by the soil covering-pressing wheel on the soil can be expressed by the following equation.

$$F = G\sin\alpha + F_N\cos\beta\sin\alpha \tag{20}$$

where, $F_N = -kx$, G is the gravity of the soil covering-pressing wheel and its appendages, N; F_N is the spring pressure, N; α is the angle between the soil covering-pressing wheel and the X axis (horizontal direction), (°); β is the angle between the mulching ballast wheel and the Z axis (forward direction), (°); k is the coefficient of elasticity, N/m; x is the deformation, m.

The agronomic requirements for the compacting strength after dry-direct-seeding of rice are generally 30-50 kPa, the requirements for soil bulk weight are 0.8-1.2 g/cm^3, and the thickness of the mulch above the seeds is 2 to 3 cm.

4 Test conditions and methods

4.1 Test conditions and instrumentation

Field performance testing and trial evaluation were conducted at the Academy of Agricultural Sciences, Harbin, Heilongjiang Province, China, in May 2021-June 2021. The previous crop in the test area was rice and the soil type was a typical black clay loam with a fine, flat soil. The thickness of the crumbly layer was 6 cm, the soil moisture content was 23% and the average firmness of the soil was 1.1 MPa. Each section of the test area is 60 m long, of which the first 10 m is the test commissioning area (data for reference only), the middle 40 m is the test testing area and the last 10 m is the test adjustment area (data for calibration only).

Test equipment: one tractor, one force tester, one SZ-1 digital soil hardness tester, one TZS-I soil moisture content tester, one GSI-200 electronic balance, one ploughing depth ruler, one electronic stopwatch, one tape measure, one ploughing depth ruler and several marking rods.

4.2 Test method

The forward speed, pressing roller diameter and compacting strength were selected as the test influencing factors, and a three-factor, five-level quadratic rotational orthogonal test design was chosen based on the factor levels. Factor level codes are listed in Table 1 and data were analyzed using Design-Expert software.

Table 1 Factor level coding table

Code value	Test factors		
	Forward speed x_1/km·h^{-1}	Pressing roller diameter x_2/mm	Compacting strength x_3/kPa
+1.682	4	370	30
+1	5	385	35
0	6	400	40
−1	7	415	45
−1.682	8	430	50

4.3 Test methods of test indicators

In accordance with the relevant provisions of the National Recommended Standard GB/T 6973-2005 of the People's Republic of China and the Agricultural Machinery Promotion and Certification Standard DG/T 083 2021. In this test, seed breakage rate, sowing depth qualification rate, coefficient of variation of sowing uniformity (measured at strip sowing) and hole grain count qualification rate (measured at hole sowing) were used as response indicators.

Seed breakage rate: Three data collection zones of 1 m in length were selected within the test area, and the total mass of rice seeds discharged from each data collection zone and the mass of broken, damaged or injured rice seeds were determined separately. The percentage of broken, damaged or injured rice seed mass to the total rice seed mass is calculated according to the following equation, and the arithmetic mean of the three measurements is taken as the seed breakage rate for the group.

$$y_1 = \frac{1}{3}\sum_{i=1}^{3}\left(\frac{m_{pi}}{m_{zi}} \times 100\%\right) \tag{21}$$

where, y_1 is seed breakage rate, %; m_{pi} is mass of broken, damaged or injured rice seeds, g; m_{zi} is total mass of rice seeds, g.

Sowing depth qualification rate: Fifty locations were selected in the test area and the thickness of the upper soil cover on the seeds was determined as the sowing depth. The sowing depth qualification rate was calculated according to the following equation (qualified sowing depth is 2-3 cm).

$$y_2 = \frac{B_h}{B_z} \times 100\% \tag{22}$$

where, y_2 is the sowing depth qualification rate, %; B_h is the number of sowing depth qualified; B_z is total number of samples.

Hole qualification rate: Three 1m long data collection zones were selected within the trial test area and the number of holes qualifying for the number of holes and the total number of holes in each data collection zone were determined separately. The percentage of holes with a qualified number of grains to the total number of holes is calculated according to the following equation, and the arithmetic mean of the three measurements is taken as the percentage of holes with a qualified number of grains for the combination (5 to 7 seeds per seed hole is a qualified hole).

$$y_3 = \frac{1}{3}\sum_{i=1}^{3}\left(\frac{S_h}{S_z} \times 100\%\right) \tag{23}$$

where, y_3 is the hole qualified rate, %; S_h is the number of holes qualified; S_z is the total number of holes.

Coefficient of variation of sowing uniformity: Twenty locations were selected in the test area and the number of seeds in each location was measured to calculate the coefficient of variation of sowing uniformity according to the following equation.

$$y_4 = \frac{\sqrt{\left[\sum_{i=1}^{n}\left(L_i - \sum_{i=1}^{n}L_i/n\right)^2\right]/(n-1)}}{\left(\sum_{i=1}^{n}L_i\right)/n} \times 100\% \tag{24}$$

where, y_4 is the coefficient of variation of sowing uniformity, %; L_i is the number of seeds; n is the number of samples.

5 Test results and analysis

5.1 Test results

In this test, the coded values for the level of each influencing factor were used as the independent variables and the seed breakage rate, sowing depth pass rate, coefficient of variation in sowing uniformity and hole qualification rate were used as the dependent variables. The test scheme and results are listed in Table 2. The trial process and rice growth are shown in Figure 7.

Table 2 Experimental design and test results

Test No.	Test factors			Response indicators			
	x_1/km·h^{-1}	x_2/mm	x_3/kPa	y_1/%	y_2/%	y_3/%	y_4/%
1	–1	–1	–1	1.15	75.16	7.99	86.78
2	1	–1	–1	1.56	77.35	8.46	86.35
3	–1	1	–1	0.93	83.47	9.02	85.68
4	1	1	–1	1.42	84.12	9.37	86.32
5	–1	–1	1	1.38	80.52	8.06	88.89
6	1	–1	1	1.63	81.22	8.42	88.12
7	–1	1	1	1.22	87.63	9.76	86.02
8	1	1	1	1.58	89.32	9.84	88.48
9	–1.682	0	0	1.12	88.95	8.47	86.36
10	1.682	0	0	1.33	90.63	9.98	88.52
11	0	–1.682	0	1.43	76.14	7.98	87.32
12	0	1.682	0	1.31	91.68	10.06	86.86
13	0	0	–1.682	0.96	76.58	7.89	86.93
14	0	0	1.682	1.39	85.37	8.62	88.85
15	0	0	0	1.49	88.96	8.05	87.45
16	0	0	0	1.55	89.81	8.13	87.85
17	0	0	0	1.54	88.32	8.16	87.98
18	0	0	0	1.68	88.98	8.05	87.03
19	0	0	0	1.58	89.14	8.10	87.32
20	0	0	0	1.53	88.65	8.11	87.58

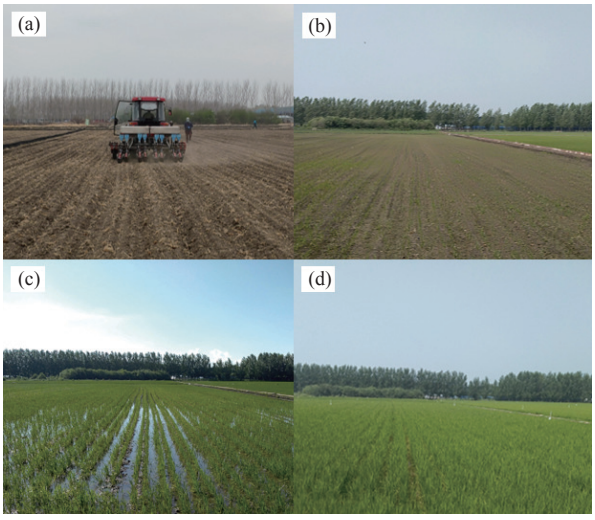

a. Field trial b. Rice emergence 30 d after sowing c. Rice emergence 60 d after sowing d. Rice emergence 80 d after sowing.

Figure 7 Trial process and rice growth

5.2 Regression analysis of the test results

Based on the test results in Table 2, the test data was processed using Design-Expert software to produce an analysis of variance (ANOVA) for the effects of forward speed, Pressing roller diameter and Compacting strength on seed breakage rate, Sowing depth qualification rate, coefficient of variation in sowing uniformity and hole qualification rate. The results of the analysis are listed in Table 3.

(1) Regression modeling and significance testing of the seed breakage rate

According to the results of the ANOVA on seed breakage rate

in Table 3, factors x_1, x_3 and x_3^2 had a highly significant effect on seed breakage rate at confidence level α=0.01, factor x_1^2 was significant at confidence level α=0.05 and the other factors were not significant. The influence of each factor on the significance of seed breakage rate was in the order of forward speed, compacting strength and pressing roller diameter. A quadratic multiple regression was fitted to the data in Table 2 to establish a quadratic regression equation for seed breakage rate.

Table 3 Analysis of variance for the effect of factors on response indicators

Source	Seed breakage rate					Sowing depth qualification rate					Sowing depth qualification rate					Hole qualification rate				
	Sum of squares	df	Mean square	F value	p value	Sum of squares	df	Mean square	F value	p value	Sum of squares	df	Mean square	F value	p value	Sum of squares	df	Mean square	F value	p value
Model	0.7604	9	0.0845	6.57	0.0035**	556.4	9	61.82	21.31	< 0.0001**	1.6	9	0.1783	27.32	< 0.0001**	14.29	9	1.59	5.83	0.0055**
x_1	0.2542	1	0.2542	19.77	0.0012**	3.47	1	3.47	1.2	0.2998	0.5648	1	0.5648	86.57	< 0.0001**	2.24	1	2.24	8.23	0.0167*
x_2	0.0436	1	0.0436	3.39	0.0953	275.85	1	275.85	95.1	< 0.0001**	0.3573	1	0.3573	54.77	< 0.0001**	1.43	1	1.43	5.24	0.0451*
x_3	0.1589	1	0.1589	12.36	0.0056**	72.05	1	72.05	24.84	0.0006**	0.4363	1	0.4363	66.87	< 0.0001**	6.76	1	6.76	24.82	0.0006**
x_1x_2	0.0045	1	0.0045	0.351	0.5667	1.19	1	1.19	0.4114	0.5357	0.045	1	0.045	6.9	0.0253*	2.31	1	2.31	8.48	0.0155*
x_1x_3	0.0105	1	0.0105	0.8178	0.3871	0.1326	1	0.1326	0.0457	0.835	0.045	1	0.045	6.9	0.0253*	0.2738	1	0.2738	1.01	0.3397
x_2x_3	0.0028	1	0.0028	0.2188	0.65	0.1326	1	0.1326	0.0457	0.835	0.045	1	0.045	6.9	0.0253*	0.2381	1	0.2381	0.8738	0.3719
x_1^2	0.1262	1	0.1262	9.82	0.0106*	0.1002	1	0.1002	0.0346	0.8562	0.0447	1	0.0447	6.86	0.0256*	0.1933	1	0.1933	0.7094	0.4193
x_2^2	0.0258	1	0.0258	2.01	0.1869	74.15	1	74.15	25.56	0.0005**	0.0209	1	0.0209	3.2	0.1041	0.8269	1	0.8269	3.04	0.1121
x_3^2	0.1784	1	0.1784	13.88	0.0039**	145.62	1	145.62	50.2	< 0.0001**	0.0365	1	0.0365	5.6	0.0395*	0.027	1	0.027	0.0992	0.7593
lack of fit	0.1075	5	0.0215	5.1	0.0526	21.05	5	4.21	2.65	0.1547	0.0369	5	0.0074	1.3	0.3895	2.12	5	0.4233	3.48	0.0985
pure error	0.0211	5	0.0042			7.96	5	1.59			0.0283	5	0.0057			0.6078	5	0.1216		
Cor total	0.889	19				585.4	19				1.67	19				17.01	19			

$$y_1 = 1.52 + 0.1364x_1 + 0.1079x_3 - 0.0894x_1^2 - 0.1071x_3^2 \quad (25)$$

(2) Regression modeling and significance testing of the sowing depth qualification rate

According to the ANOVA results in Table 3, factors x_2, x_3, x_2^2 and x_3^2 had a highly significant effect on the sowing depth qualification rate at confidence level $\alpha = 0.01$, while the other factors were not significant. The influence of each factor on the significance of sowing depth qualification rate was in the order of pressing roller diameter, compacting strength and forward speed. A quadratic multiple regression was fitted to the data in Table 2 to establish a quadratic regression equation for the sowing depth qualification rate.

$$y_2 = 88.07 + 4.49x_2 + 2.30x_3 - 2.26x_2^2 - 3.17x_3^2 \quad (26)$$

(3) Regression modeling and significance testing for the coefficient of variation in sowing uniformity

According to the ANOVA results in Table 3, factors x_1, x_2 and x_3 have a highly significant effect on the coefficient of variation of sowing uniformity at confidence level $\alpha = 0.01$, factors x_1x_2, x_1x_3, x_2x_3, x_1^2 and x_2^2 are significant at confidence level $\alpha = 0.05$, while the other factors are not significant. The influence of each factor on the significance for the coefficient of variation in sowing uniformity was in the order of forward speed, compacting strength and pressing roller diameter. A quadratic multiple regression was fitted to the data in Table 2 to establish a quadratic regression equation for the coefficient of variation in sowing uniformity.

$$y_3 = 4.15 + 0.2034x_1 - 0.1618x_2 + 0.1787x_3 + 0.0750x_1x_2 + 0.0750x_1x_3 + 0.0750x_2x_3 - 0.0519x_1^2 + 0.0541x_2^2 \quad (27)$$

(4) Regression modeling and significance testing of the hole qualification rate

According to the ANOVA results in Table 3, factors x_3 have a highly significant effect on the coefficient of variation of sowing uniformity at confidence level $\alpha = 0.01$, factors x_1, $x_2$and x_1x_2 are significant at confidence level $\alpha = 0.05$, while the other factors are not significant. The influence of each factor on the significance for the coefficient of the hole qualification rate was in the order of compacting strength, forward speed, and pressing roller diameter. A quadratic multiple regression was fitted to the data in Table 2 to establish a quadratic regression equation of the hole qualification rate.

$$y_4 = 87.33 + 0.4051x_1 - 0.3232x_2 + 0.7036x_3 + 0.5375x_1x_2 \quad (28)$$

5.3 Analysis and optimisation of response surface

5.3.1 Response surface analysis of the seed breakage rate

Since the diameter of the pressing roller had no significant effect on the seed breakage rate, the diameter of the pressing roller was fixed at zero level (x_2= 400 mm) to investigate the effect of forward speed and compacting strength on the seed breakage rate and their interaction. The response surface for the two-factor effect on seed breakage rate is shown in Figure 8a.

As can be seen from Figure 8, the seed breakage rate increases and then decreases with increasing forward speed at a pressing roller diameter of 400 mm, and the maximum value occurring around x_1=7.83 km/h. The seed breakage rate increases and then decreases with increasing compacting strength, and the maximum value occurring around x_3=45.02 km/h.

5.3.2 Response surface analysis of the sowing depth qualification rate

Since the forward speed had no significant effect on the sowing depth qualification rate, the forward speed was fixed at zero level (x_1=6 km/h) to investigate the effect of pressing roller diameter and compacting strength on the sowing depth qualification rate and their interaction. The response surface for the two-factor effect on the sowing depth qualification rate is shown in Figure 8b.

As can be seen from Figure 9, at a forward speed of 6 km/h, the sowing depth qualification rate increases with the diameter of the pressing roller , and the maximum value occurs around x_2=430 mm. The sowing depth qualification rate increases and then decreases with increasing compacting strength, and the maximum value occurs around x_3=43.62 kPa.

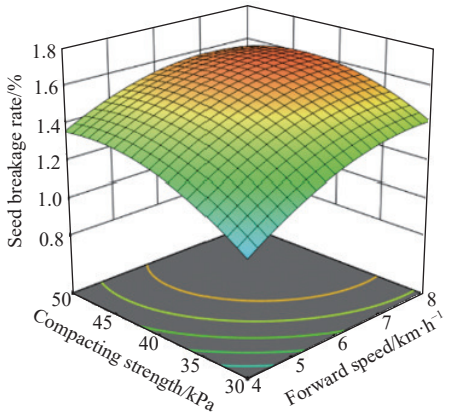

a. Seed breakage rate

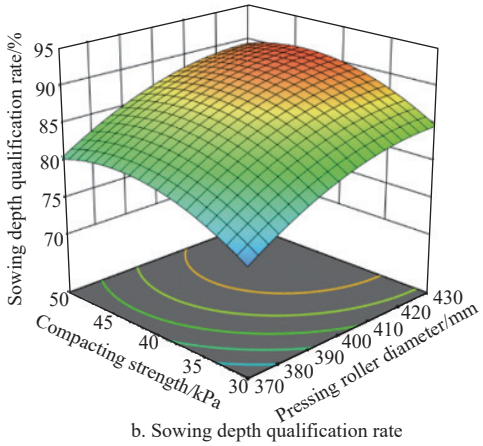

b. Sowing depth qualification rate

Figure 8 Response surface plots of the seed breakage rate and sowing depth qualification rate

5.3.3 Response surface analysis of the coefficient of variation in sowing uniformity

Fixing any of the three factors of the regression model at the zero level and examining the effect of the other two factors on the coefficient of variation in sowing uniformity and their interaction. The response surface for the effect of each factor on the coefficient of variation in sowing uniformity is shown in Figure 9.

As can be seen from Figure 9a, the coefficient of variation in sowing uniformity increases with increasing forward speed and decreases with increasing pressing roller diameter at a compacting strength of 40 kPa. As can be seen from Figure 9b, the coefficient of variation in sowing uniformity increases with increasing forward speed and with increasing compacting strength at a pressing roller diameter of 400 mm. As can be seen from Figure 9c, at a forward speed of 6 km/h, the coefficient of variation in sowing uniformity decreases with increasing diameter of the pressing roller and increased with increasing compacting strength.

5.3.4 Response surface analysis of the hole qualification rate

Fixing any of the three factors of the regression model at the zero level and examining the effect of the other two factors on the hole qualification rate and their interaction. The response surface for the effect of each factor on the hole qualification rate is shown in Figure 10.

From Figure 10a, it can be seen that under the compacting strength of 40 kPa, the forward speed of 4.0-7.2 km/h and the diameter of the pressing roller s of 370-377.4 mm, the hole qualification rate decreases with the increase of the forward speed and decreases with the increase of the diameter of the pressing roller; when the forward speed is 4-7.2 km/h and the diameter of the pressing roller is 377.4-430 mm, the hole qualification rate

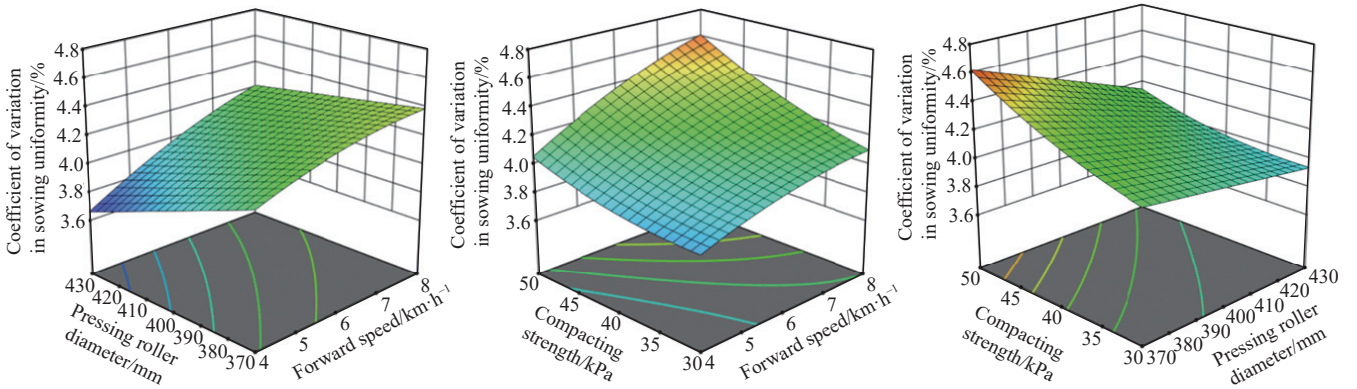

a. Pressing roller diameter and forward speed b. Compacting strength and forward speed c. Compacting strength and pressing roller diameter

Figure 9 Response surface plots of different factors on coefficient of variation in sowing uniformity

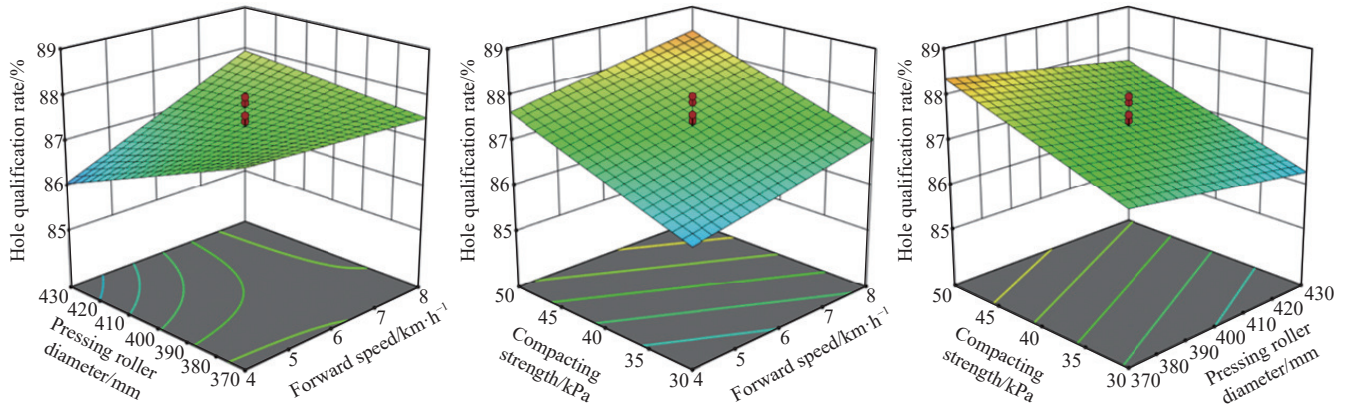

a. Pressing roller diameter and forward speed b. Compacting strength and forward speed c. Compacting strength and pressing roller diameter

Figure 10 Response surface plots of different factors on hole qualification rate

increases with the increase of forward speed and decreases with the increase of diameter of the pressing roller; when the forward speed is 7.2-8 km/h and the diameter of the pressing roller is 370-377.4 mm, the hole qualification rate decreases with the increase of forward speed and increases with the increase of diameter of the pressing roller; when the forward speed is 7.2-8 km/h and the diameter of the pressure roller is 370-377.4 mm, the hole qualification rate decreases with the increase of forward speed and increases with the increase of diameter of the pressing roller . From Figure 10b, it can be seen that under the condition that the diameter of the pressing roller is 400 mm, the hole qualification rate increases with the increase of the forward speed and increases with the increase of the compacting strength. As can be seen from Figure 10c, at a forward speed of 6 km/h, the hole qualification rate decreases with the increase in pressing roller diameter and increases with the increase in compacting strength.

5.4 Optimisation of the test programme

According to the promotion and appraisal standard of DG/T 0832021 direct seeding machine for rice, the following optimization constraints were selected, taking into account the actual working conditions, agronomic technical requirements and the analysis of test results.

$$\begin{cases} \min y_1\ (0\% \le y_1 \le 1.5\%) \\ \max y_2\ (85\% \le y_2 \le 100\%) \\ \min y_3\ (0\% \le y_3 \le 4.5\%) \\ \max y_4\ (85\% \le y_4 \le 100\%) \\ 4\ \text{km/h} \le x_1 \le 8\ \text{km/h} \\ 370\ \text{mm} \le x_2 \le 430\ \text{mm} \\ 30\ \text{kPa} \le x_3 \le 50\ \text{kPa} \end{cases} \tag{29}$$

The main objective function optimization method was used and optimized by the Design-Expert software to produce a better test solution. The optimum solution was determined according to the actual operating conditions and the detailed parameter combinations are listed in Table 4.

Table 4 Optimal combination of parameters

x_1/km·h^{-1}	x_2/mm	x_3/kPa	y_1/%	y_2/%	y_3/%	y_4/%
4	427	48.45	1.31	89.95	3.75	86.75

5.5 Verification test

Different measurement areas of the same plot were selected and verification tests were carried out according to the optimal combination of parameters, and the test photos are shown in Figure 11. The Verification results showed that the optimal combination for dry-direct-seeding for rice in cold regions resulted in a seed breakage rate of 1.35%, a sowing depth qualification rate of 90.22%, a coefficient of variation in sowing uniformity of 3.79% and a hole qualification rate of 86.88%. Comparison with the results of the quadratic regression orthogonal rotational combination test showed that the results of the verification test were similar to the results of the experimental analysis. This indicates that the planting unit for rice dry-direct-seeding planter in cold regions designed in this paper meets the design requirements.

Figure 11 Field verification trial

6 Conclusions

(1) In this paper, a planting unit for rice dry-direct-seeding in cold regions was designed. This sowing unit used pressing rollers to open the furrow, combined strip and hole sowing, and employed a self-rotating extruding soil covering-pressing device with a soil breaking function for soil compaction. These design features effectively addressed the challenges faced during the dissemination of dry-direct-seeding technology for rice in northeast China.

(2) A three-factor, five-level quadratic rotational orthogonal combination test was arranged by analyzing the kinematics and working conditions of the key components. Regression modeling was established between each test index and the influencing factors. The effects of forward speed, pressing roller diameter, and compacting strength on seed breakage rate, sowing depth qualification rate, coefficient of variation in sowing uniformity, and hole qualification rate were analyzed.

(3) The factors that had a significant effect on the seed breakage rate were, in order of significance: forward speed, compacting strength, and pressing roller diameter. The factors that significantly affected the sowing depth qualification rate were, in order of significance: pressing roller diameter, compacting strength, and forward speed. The factors influencing the significance of the coefficient of variation in sowing uniformity were, in order of significance: forward speed, compacting strength, and pressing roller diameter. The factors that had a significant impact on the hole qualification rate were, in order of significance: compacting strength, forward speed, and the diameter of the pressing roller.

(4) According to the regression model, the parameters were optimized and the analysis yielded the optimal combination of parameters: forward speed 4 km/h, pressing roller diameter 427 mm and compacting strength 48.45 kPa, at this point the seed breakage rate was 1.31%, the sowing depth qualification rate was 89.95%, the coefficient of variation in sowing uniformity was 3.75% and the hole qualification rate was 86.75%. The verification test results differed little from the optimized values, which are accurate and reliable, and this meets the agronomic requirements of dry-direct-seeding.

Acknowledgements

We acknowledged that the research was financially supported by the National Natural Science Foundation of China (Nos. 52075215 and 52275250 and 52105300), Key Research and Development Program of Changchun, China (Grant No. 21ZGN22), and the Science and Technology Research Project of Jilin Provincial Education Department (No. JJKH20221021KJ).

[References]

[1] Wang B L, Luo X W, Wang Z M, Zheng L, Zhang M H, Dai Y Z, et al. Design and field evaluation of hill-drop pneumatic central cylinder direct-seeding machine for hybrid rice. Int J Agric & Biol Eng, 2018; 11(6): 33–40.

[2] Lin H I, Yu Y Y, Wen F I, Liu P T. Status of food security in East and

Southeast Asia and challenges of climate change. Climate, 2022; 10(3): 40.
[3] Ma G H, Yuan L P. Hybrid rice achievements, development and prospect in China. Journal of Integrative Agriculture, 2015; 14(2): 197–205.
[4] Zhuang Y H, Zhang L, Li S S, Liu H B, Zhai L M, Zhou F, Ye Y S, Ruan S H, Wen W J. Effects and potential of water-saving irrigation for rice production in China. Agricultural Water Management, 2019; 217: 374–382.
[5] Zhang H C, Gong J L. Research status and development discussion on high-yielding agronomy of mechanized planting rice in China. Scientia Agricultural Sinica, 2014; 47(7): 1273–1289. (in Chinese)
[6] Tao Y, Chen Q, Peng S B, Wang W Q, Nie L X. Lower global warming potential and higher yield of wet direct-seeded rice in Central China. Agronomy for Sustainable Development, 2016; 36(2): 1–9.
[7] Farooq M, Siddique K H M, Rehman H, Aziz T, Lee D, Wahid A. Rice direct seeding: Experiences, challenges and opportunities. Soil & Tillage Research, 2011; 111: 87–98.
[8] Luo X W, Liao J, Zang Y, Zhou Z Y. Improving agricultural mechanization level to promote agricultural sustainable development. Transactions of the CSAE, 2016; 32(1): 1–11 (in Chinese).
[9] Mishra A K, Khanal A R, Pede V O. Is direct seeded rice a boon for economic performance? Empirical evidence from India. Food Policy, 2017; 73: 10–18.
[10] Kumar V, Ladha J K. Direct seeding of rice: recent developments and future research needs. Advances in Agronomy. Academic Press, 2011; 111: 297–413.
[11] Zhang M H, Wang Z M, Luo X W, Zang Y, Yang W W, Xing H, et al. Review of precision rice hill-drop drilling technology and machine for paddy. Int J Agric & Biol Eng, 2018; 11(3): 1–11.
[12] Luo X W, Wang Z M, Zeng S, Zang Y, Yang W W, Zhang M H. Recent advances in mechanized direct seeding technology for rice. Journal of South China Agricultural University, 2019; 40(5): 1–13. (in Chinese)
[13] Li Z H, Ma X, Li X H, Chen L T, Li H W, Yuan Z C. Research progress of rice transplanting mechanization. Transactions of the CSAM, 2018; 49 (5): 1–20. (in Chinese)
[14] Dai Y Z, Luo Xi W, Zhang M H, Lan F, Zhou Y J. Design and experiments of the key components for centralized pneumatic rice dry direct seeding machine. Transactions of the CSAE, 2020; 36(10): 1–8. (in Chinese)
[15] Wang Z M, Pei J, He J, Zhang M G, Yang M M. Development of the sowing rate monitoring system for precision rice hill-drop drilling machine. Transactions of the CSAE, 2020; 36(10): 9–16. (in Chinese)
[16] Liu C L, Li Y N, Song J N, Zhang F Y, Wei D, Zheng S X. Simulation design and experiment of a directional seed-feeding device. International Agricultural Engineering Journal, 2017; 26(4): 16–24.
[17] Zhang Y P, Du R C, Diao P S Yang S D. Experiment of no-tillage and drought direct sowing rice and feasibility analysis in Shandong Province. Transactions of the CSAE, 2016; 32(12): 24–30. (in Chinese)
[18] Zhang G Z, Luo X W, Zang Y, Wang, Z M, Zeng S, Zhou Z Y. Experiment of sucking precision of sucking plate with group holes on rice pneumatic metering device. Transactions of the CSAE, 2013; 29(6): 13–20. (in Chinese)
[19] Zhang M H, Wang Z M, Luo X W, Yang W W, Dai Y Z, Wang B L. Design and experiment of furrowing device of precision hill-drop drilling machine for rice. Transactions of the CSAE, 2017; 33(5): 10–15. (in Chinese)
[20] Xing H, Zang Y, Wang Z M, Luo X W, Pei J, He S Y, et al. Design and parameter optimization of rice pneumatic seeding metering device with adjustable seeding rate. Transactions of the CSAE, 2019; 35(4): 20–28. (in Chinese)
[21] Zhang M H, Luo X W, Wang Z M, Dai Y Z, Wang B L, Zheng L. Design and experiment of combined hole-type metering device of rice hill-drop drilling machine. Transactions of the CSAM, 2016; 47(9): 29–36. (in Chinese)
[22] Luo X W, Liu T, Jiang E C, Li Q. Design and experiment of hill sowing wheel of precision rice direct seeder. Transactions of the CSAE, 2007; 23(3): 108–112. (in Chinese)
[23] Wang J W, Zhou W Q, Tian L Q, Li S W, Zhang Z. Virtual simulation analysis and verification of seed-filling mechanism for dipper hill-drop precision direct rice seeder. Int J Agric & Biol Eng, 2017; 10(6): 77–85.
[24] Xing H, Wang Z M, Luo X W, Cao X M, Liu C B, Zang Y. General structure design and field experiment of pneumatic rice direct-seeder. Int J Agric & Biol Eng, 2017; 10(6): 31–42.
[25] Wang Z M, Huang Y C, Wang B L, Zhang M H, Ma Y X, Ke X R, et al. Design and experiment of rice precision metering device with sowing amount stepless adjusting. Transactions of the CSAE, 2018; 34(11): 9–16. (in Chinese)
[26] Liu C L, Wang Y L, Du X, Song J N, Wang J H, Zhang F Y. Filling performance analysis and verification of cell-belt rice precision seed-metering based on friction and repeated filling principle. Transactions of the CSAE, 2019; 35(4): 29–36. (in Chinese)
[27] Lv X R, Lv X L, Ren W T. Experimental Study on Working Performance of Rice Rope Direct Seeding Machine. Agricultural Sciences in China 2010; 9(2): 275–279.
[28] Ma J, Lei X L, Ma R C. Structural design and parameters optimization of rice seed-metering device. Applied Mechanics and Materials, 2013; 397: 957–965.
[29] Tian L Q, Wang J W, Tang H, Li S W, Zhou W Q, Shen H G. Design and performance experiment of helix grooved rice seeding device. Transactions of the CSAM, 2016; 47(5): 46–52. (in Chinese)